COMPUTATIONAL MECHANICS 2022
37th conference with international participation
Srní
November 7 - 9, 2022

On the development of Cahn-Hilliard Navier-Stokes numerical solver within OpenFOAM framework

J. Musil

Faculty of Mechanical Engineering, Czech Technical University in Prague, Karlovo nám. 13, 121 35 Praha, Czech Republic

1. Introduction

One of the most common approach used in engineering applications dealing with two-phase fluid flows is Volume-of-Fluid (VoF) method. The VoF method consists of the Navier-Stokes equations equipped with transport equation for phase interface capturing indicator function. Although the VoF method experienced considerable improvements of numerical algorithms over the years, still it relies on artificially introduced features like interface compression term or algorithmically complex geometric interface reconstruction numerical schemes.

An alternative, less common approach refers to diffuse interface models, often labeled as Cahn-Hilliard models. Those models track the interface of two phases using a smooth phase-field function allowing a diffuse transition between the physical properties from one phase to the other and circumvents modeling the jump discontinuities at the interface. The Cahn-Hilliard equations exhibit many advantages, including mass conservation, thermodynamic consistency, and a free-energy based description of surface tension with a well-established theory from non-equilibrium thermodynamics.

Moreover, Cahn-Hilliard model combined with Navier-Stokes equations can be in fact regarded as a VoF model augmented by non-linear, fourth-order diffusive term which naturally incorporates surface tension and possibly allows under-resolving of flow field in regions of less importance, thus reduction of computational time. On the other hand, the system of equations is even more strongly coupled which pose challenging issue to design efficient, provably energy-stable and ideally decoupled numerical algorithms.

The contribution presents Cahn-Hilliard Navier-Stokes (CHNS) solver being developed within the OpenFOAM framework [4]. The aim of this endeavor is to provide efficient and robust solver of two-phase fluid flows integrated in popular OpenFOAM package already equipped with adaptive-mesh-refinemet and parallelization tools. The attention is paid to the description of two possible versions of numerical algorithms utilizing block-coupling framework introduced in OpenFOAM-extend. The performance of new solvers is compared with OpenFOAM native VoF solver on a simple test case. Some possible phase-field model adjustments and modifications are outlined and future development directions are discussed.

2. Mathematical models

The VoF model is described as follows. It consists of Eq. (1)–(3), where $0 \leq \alpha \leq 1$ is the indicator function (liquid fraction in the mixture) and the property of the mixture is calculated as $\chi = \alpha\chi_1 + (1-\alpha)\chi_2$ with χ here being substituted density ρ and dynamic viscosity η and χ_1, χ_2 representing values of unmixed phases. The deviatoric stress tensor $\boldsymbol{\tau} = \eta(\alpha)[\boldsymbol{\nabla u} + (\boldsymbol{\nabla u})^T]$

expresses tangential stresses, $\boldsymbol{g}$ is the acceleration due to gravity, σ is the surface tension and $\kappa = -\boldsymbol{\nabla} \cdot (\boldsymbol{\nabla}\alpha/|\boldsymbol{\nabla}\alpha|)$ is the surface curvature. The dynamic pressure and volume-averaged velocity of the mixture are denoted by p_d and $\boldsymbol{u}$, respectively.

$$\partial_t(\rho\boldsymbol{u}) + \boldsymbol{\nabla} \cdot (\rho\boldsymbol{u} \otimes \boldsymbol{u}) + \boldsymbol{\nabla} p_d - \boldsymbol{\nabla} \cdot \boldsymbol{\tau} + (\boldsymbol{g} \cdot \boldsymbol{x})\boldsymbol{\nabla}\rho - \sigma\kappa\boldsymbol{\nabla}\alpha = \boldsymbol{0}, \tag{1}$$

$$\boldsymbol{\nabla} \cdot \boldsymbol{u} = 0, \tag{2}$$

$$\partial_t\alpha + \boldsymbol{\nabla} \cdot (\alpha\boldsymbol{u}) = 0. \tag{3}$$

The second considered model, the phase-field formulation, is represented by the system of Cahn-Hilliard Navier-Stokes equations which reads (for detailed derivation of the model, see e.g. [1])

$$\partial_t(\rho\boldsymbol{u}) + \boldsymbol{\nabla} \cdot (\rho\boldsymbol{u} \otimes \boldsymbol{u}) + \nabla \cdot (\boldsymbol{u} \otimes \boldsymbol{J}) + \boldsymbol{\nabla} p_d - \boldsymbol{\nabla} \cdot \boldsymbol{\tau} + (\boldsymbol{g} \cdot \boldsymbol{x})\boldsymbol{\nabla}\rho + \varphi\boldsymbol{\nabla}\mu = \boldsymbol{0}, \tag{4}$$

$$\boldsymbol{J} = \frac{\rho_2 - \rho_1}{2} M(\varphi)\boldsymbol{\nabla}\mu, \tag{5}$$

$$\boldsymbol{\nabla} \cdot \boldsymbol{u} = 0, \tag{6}$$

$$\partial_t\varphi + \boldsymbol{\nabla} \cdot (\varphi\boldsymbol{u}) - \boldsymbol{\nabla} \cdot (M(\varphi)\boldsymbol{\nabla}\mu) = 0, \tag{7}$$

$$\left.\begin{aligned} \mu &= \frac{\sigma}{\epsilon}F'(\varphi) - \sigma\epsilon\Delta\varphi \\ F(\varphi) &= \frac{1}{4}(\varphi^2 - 1)^2 \end{aligned}\right\} \longrightarrow\ \mu = \frac{\sigma}{\epsilon}(\varphi^3 - \varphi) - \sigma\epsilon\Delta\varphi. \tag{8}$$

Here $-1 \leq \varphi \leq 1$ is the phase-field function and the density of the mixture is calculated as $\rho = \frac{\rho_1 - \rho_2}{2}\varphi + \frac{\rho_1 + \rho_2}{2}$. The dynamic viscosity is calculated similarly. The deviatoric stress tensor, dynamic pressure and volume-averaged velocity of the mixture are $\boldsymbol{\tau}$, p_d and $\boldsymbol{u}$, respectively. The $\boldsymbol{J}$ represents mass diffusion due to the concentration differences at the phase interface, μ is chemical potential function, $F(\varphi)$ is the bulk free energy potential function, σ is the surface tension, ϵ is parameter proportional to the interface thickness, $M(\varphi)$ is the mobility parameter.

3. Numerical algorithms

3.1 interFoam

As the reference for newly developing phase-field based algorithm, the OpenFOAM solver *interFoam* based on VoF model is chosen. The solver relies on a pressure-velocity coupling PISO algorithm when solving Eq. (2)–(3) in addition with solving the Eq. (1) which is achieved by means of the MULES explicit solver based on the FCT technique. The detailed description can be found in e.g. [3].

3.2 chnsCoupledFiMuFoam

In the first variant of presented phase-field algorithm Eq. (9)–(10) are substituted in the Eq. (3) in the original *interFoam* solver. The Eq. (9)–(10) are solved by means of block-matrix coupling framework available in foam-extend fork. The variables in $[\cdot]^{n+1}$ are solved implicitly, while the ones in $(\cdot)^{n+1}$ are updated by iterative loop. Then PISO algorithm for updating pressure and velocity follows.

$$\frac{[\varphi]^{n+1} - \varphi^n}{\delta t} + \boldsymbol{\nabla} \cdot ([\varphi]^{n+1}\boldsymbol{u}^n) - \boldsymbol{\nabla} \cdot (M(\varphi^{n+1})\boldsymbol{\nabla}[\mu]^{n+1}) = 0, \tag{9}$$

$$[\mu]^{n+1} = \frac{\sigma}{\epsilon}\Big((\varphi^{n+1})^2 - 1\Big)[\varphi]^{n+1} - \sigma\epsilon\Delta[\varphi]^{n+1}. \tag{10}$$

3.3 chnsCoupledFiMuPdFoam

The second variant of the phase field algorithm uses slightly modified pressure-velocity decoupled approach proposed in [2]. The system of Eq. (11)–(14) is solved by block-matrix coupling till congvergence is reached. Then, with use of updated mass flux of Eq. (15) the momentum equation (16) is solved only once.

$$\frac{[\varphi]^{n+1}-\varphi^n}{\delta t}+\boldsymbol{\nabla}\cdot([\varphi]^{n+1}\boldsymbol{u}_*)-\boldsymbol{\nabla}\cdot(M(\varphi^{n+1})\boldsymbol{\nabla}[\mu]^{n+1})=0, \tag{11}$$

$$\boldsymbol{u}_*=\frac{\rho^n\boldsymbol{u}^n}{\rho^{n+1}}-\frac{\delta t}{\rho^{n+1}}\Big(\varphi^{n+1}\boldsymbol{\nabla}[\mu]^{n+1}+\boldsymbol{\nabla}[p_d]^{n+1}+(\boldsymbol{g}\cdot\boldsymbol{x})\boldsymbol{\nabla}[\varphi]^{n+1}\Big), \tag{12}$$

$$\boldsymbol{\nabla}\cdot\boldsymbol{u}_*=0, \tag{13}$$

$$[\mu]^{n+1}=\frac{\sigma}{\epsilon}((\varphi^{n+1})^2-1)[\varphi]^{n+1}-\sigma\epsilon\Delta[\varphi]^{n+1}, \tag{14}$$

$$\boldsymbol{J}^{n+1}=\frac{\rho_2-\rho_1}{2}M(\varphi^{n+1})\boldsymbol{\nabla}\mu^{n+1}, \tag{15}$$

$$\frac{\rho^{n+1}[\boldsymbol{u}]^{n+1}-\rho^{n+1}\boldsymbol{u}_*}{\delta t}+\boldsymbol{\nabla}\cdot(\rho^{n+1}\boldsymbol{u}_*\otimes[\boldsymbol{u}]^{n+1})+\boldsymbol{\nabla}\cdot(\boldsymbol{u}_*\otimes\boldsymbol{J}^{n+1})-\boldsymbol{\nabla}\cdot[\boldsymbol{\tau}]^{n+1}=0. \tag{16}$$

4. Numerical results

Both two above mentioned versions of CHNS algorithms were tested on the simple 2D case of two collapsing water droplets. The computational domain is a square $\Omega=[0,0.1]^2$. The droplets of radii $r=0.01$ m are each distanced from the domain center horizontally by 0.025 m. The droplets are collapsed together by opposite horizontal velocities of magnitude $|\boldsymbol{u}|=0.05$ m/s. The boundary conditions were set as: $\boldsymbol{u}=\boldsymbol{0}$, $\boldsymbol{\nabla}p_d\cdot\boldsymbol{n}=0$, $\boldsymbol{\nabla}\varphi\cdot\boldsymbol{n}=0$, $\boldsymbol{\nabla}\mu\cdot\boldsymbol{n}=0$. The parameters in the model are chosen as $\rho_1=1\,\mathrm{kg/m^3}$, $\rho_2=10^3\,\mathrm{kg/m^3}$, $\eta_1=10^{-3}$ Pa·s, $\eta_2=1.8\times10^{-5}$ Pa·s. The surface tension is set as $\sigma=0.07\,\mathrm{kg/s^2}$ and interface thickness $\epsilon=10^{-3}$ m. The mobility parameter was considered constant: $M(\varphi)=M=10^{-6}\,\mathrm{kg^{-1}m^3s^{-1}}$. The gravity was not taken into account and the fluid flow was considered laminar. As a reference, the case was also computed with *interFoam* solver with the same corresponding physical parameters and boundary conditions ($\boldsymbol{\nabla}\alpha\cdot\boldsymbol{n}=0$).

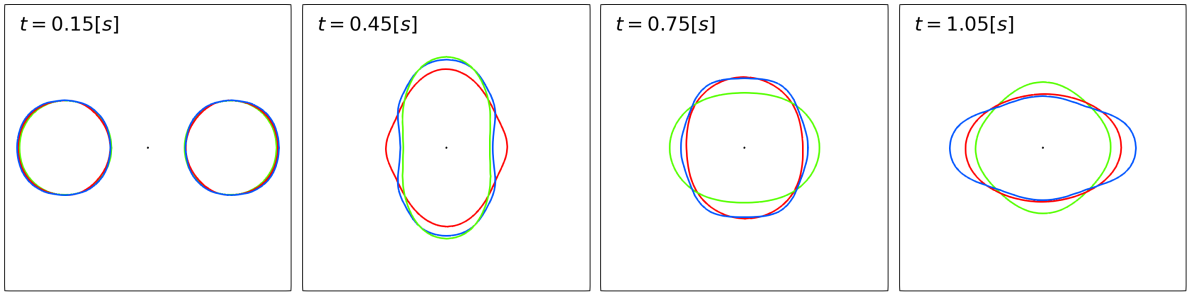

Fig. 1. Time evolution of collapsing droplets. The detail of (0.06×0.06) m centered square region of the original domain shows the contours of $\rho=500\,\mathrm{kg/m^3}$ (phase interface) for the solutions obtained by: • *interFoam* , • *chnsCoupledFiMuFoam*, • *chnsCoupledFiMuPdFoam*

In Fig. 1, one can see amplifying difference in the oscillating droplet shapes during the time. It has been found out that values of the mobility parameter M and the length parameter ϵ can have strong influence on the stability and speed of computations as well as the dynamics of the system.

In Fig. 2, there are plotted graphs of the relative total energy $\mathcal{E}_r(t) = \mathcal{E}(t)/\mathcal{E}(0)$, where $\mathcal{E}(t)$ being sum of total kinetic energy, gravitational potential energy and total free energy. The graphs suggest that *chnsCoupledFiMuPdFoam* performs better in the energy dissipation rate than *chnsCoupledFiMuFoam* while *interFoam* exhibits large oscillations in the total energy. This is probably caused by incompletely defined total free energy used for VoF formulation:

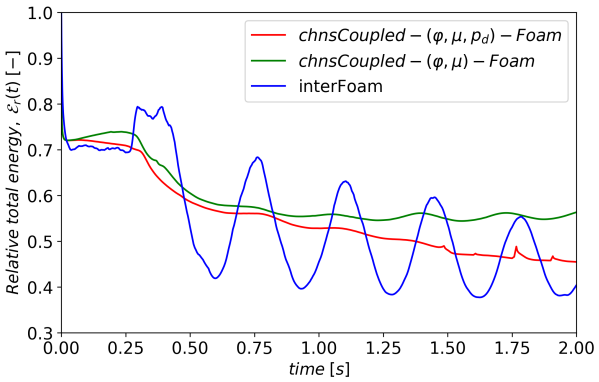

Fig. 2. Energy dissipation curves

$$\mathcal{F}_{CHNS} = \int_\Omega \left(\frac{\sigma}{\epsilon} F(\varphi) + \tfrac{1}{2}\sigma\epsilon |\boldsymbol{\nabla}\varphi|^2 \right) dx \qquad vs. \qquad \mathcal{F}_{VoF} = \int_\Omega \left(\tfrac{1}{2}\sigma\epsilon |\boldsymbol{\nabla}\alpha|^2 \right) dx \tag{17}$$

From the point of CPU efficiency, the best results were obtained by *interFoam*, up to 2 times faster than phase-field codes. But on the other hand the presented phase-field codes are sensitive to solver setting and need to be further examined and adjusted. The error of mass conservation was within 1% at the phase-field models, while at *interFoam* almost down to computer precision. The poor mass conservation of phase-field model can be caused by possibly ill posed boundary conditions.

5. Discussion

During the phase-field algorithm testing procedure it turned out that further investigation of the solver parameters setting playing crucial role in computational efficiency is needed. Future work will be focused on design of variable mobility parameter, based on grid resolution handled by adaptive-mesh-refinement and/or under-resolving flow conditions in order to fully utilize and improve the promising features of phase-field model which have not been met quite met at this stage. Other variants of coupled/segregated procedures will be considered with the aim to prove energy stability of such algorithms.

Acknowledgement

This work was supported by the Grant Agency of the Czech Technical University in Prague, grant No. SGS22/148/OHK2/3T/12.

References

[1] Abels, H., Garcke, H., Grün, G., Thermodynamically consistent, frame indifferent diffuse interface models for incompressible two-phase flows with different densities, Mathematical Models and Methods in Applied Sciences 22 (3) (2012) No. 1150013.

[2] Kou, J., Wang, X., Zeng, M., Cai, J., Energy stable and mass conservative numerical method for a generalized hydrodynamic phase-field model with different densities, Physics of Fluids 32 (11) (2020) No. 117103.

[3] Márquez Damián, S., An extended mixture model for the simultaneous treatment of short and long scale interfaces, Ph.D. thesis, National University of the Littoral, Santa Fe, 2013.

[4] Weller, H. G., Tabor, G., Jasak, H., Fureby, C., A tensorial approach to computational continuum mechanics using object-oriented techniques, Computers in Physics 12 (1998) 620-631.